URSI GASS 2021, Rome, Italy, 28 August - 4 September 2021

Design of Plasmonic Devices Using Time-Division Parallel Algorithm

Seiya Kishimoto*, Di Wu, and Shinichiro Ohnuki
College of Science and Technology, Nihon University, Tokyo, Japan

Abstract

Novel parallel algorithm is introduced for electromagnetic transient analysis in order to design plasmonic devices. We have established time-division parallel computation for the finite-difference time-domain (FDTD) method. This completely parallel technique is extremely useful, since the computational task can be equally distributed to many processors and there is no data communication during a computation. The key idea of this parallel algorithm is as follows: (i) The coarse values at temporal sampling points can be independently obtained using a finite-difference complex-frequency-domain with a fast inverse Laplace transform. (ii) These values are transferred to the initial responses of the FDTD frames in many computational processors. (iii) Conventional FDTD computation is simply performed in completely parallel. The computational time for sequential part can be reduced to a fraction of the number of processors. We will apply the proposed technique to designing a plasmonic antenna for all optical magnetic recording purpose.

1 Introduction

A novel parallel algorithm is proposed for studying electromagnetic transient responses. We have developed time-division parallel method for performing the finite-difference time-domain (FDTD) simulation efficiently [1, 2]. This technique is completely parallel and the computational time for sequential part can be reduced to a fraction of the number of processors. The basic concept of our method is shown as in Figure 1:

1) In the computational process, the task for the entire observation time is divided into many temporal periods and distributed into many processors.
2) The initial response for each temporal period is obtained by a finite-difference complex-frequency-domain with a fast inverse Laplace transform (FDCFD-FILT) [3-5]. This can be performed in completely parallel [6], since information about the previous observation time is not required.
3) The obtained initial response is transferred to the FDTD frame and conventional FDTD computation can be simply performed using many processors. This process is also completely parallel, since there is no data communication during the FDTD computation.
4) As the last step, the computational results stored in all processors are merged and the whole time-domain response can be obtained. The computational time for sequential part can be reduced to a fraction of the number of processors.

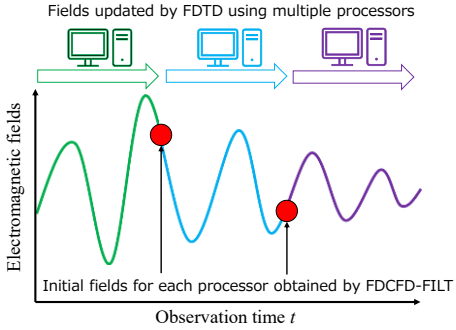

Figure 1. Basic concept of time-division parallel computing for FDTD. The instantaneous EM field is obtained by FDCFD-FILT. The time evolution of the EM field is computed by FDTD.

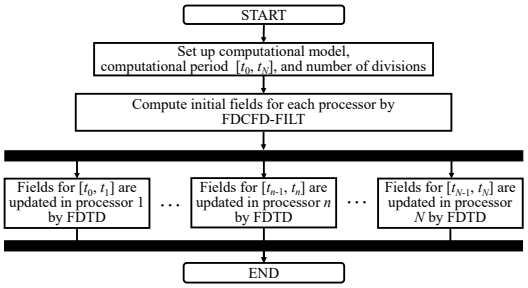

Figure 2. Flowchart for time-division parallel algorithm. Computational period is divided into processors. Each initial field is obtained by FDCFD-FILT. It is updated by FDTD.

To evaluate the reliability of our proposed method, we investigate the transient electromagnetic scattering from a metallic nanosphere. Furthermore, we apply the time-division parallel FDTD computation to designing a realistic plasmonic antenna for ultrafast magnetic recording systems [7-9].

2 Time-Division Parallel Computing

A flowchart of the proposed time-division parallel computing is shown in Figure 2. The period $[t_n\text{-}1, t_n]$ is the computational task for the n-th processor. To compute the time evolution of the electromagnetic field in the n-th processor, the initial response is computed by FDCFD-FILT. This value is transferred to the FDTD frame and perform conventional FDTD computation. Next, we briefly explain the concept of FDCFD-FILT by which the initial response of each period can be obtained.

2.1 FDCFD-FILT

The instantaneous electric field distribution $\boldsymbol{e}(t)$ at a specific observation time t can be obtained by FDCFD-FILT [3, 5]. In FDCFD, Maxwell's equation is transformed into the complex frequency domain by a Laplace transform and represented by the wave equation:

$$\nabla \times (\mu^{-1}\nabla \times \boldsymbol{E}(s)) + s^2\varepsilon\boldsymbol{E}(s) = -s\boldsymbol{J}, \quad (1)$$

where s is the complex frequency, μ is the permeability, ε is the permittivity, $\boldsymbol{J}$ is the current density, and $\boldsymbol{E}(s)$ is the unknown electric field vector in the complex-frequency domain. To solve (1), the electric field is discretized by the Yee cell. Using the finite-difference scheme on the differential operator, the linear equation form $\bar{\boldsymbol{A}}\boldsymbol{E} = \boldsymbol{J}$ can be obtained, where $\bar{\boldsymbol{A}}$ is the operator matrix. The spatial distribution of the electric field in the complex-frequency domain can be obtained by solving the linear equation [3].

The complex frequency function is transformed into time domain by FILT [4, 5]. The Bromwich integral is represented by the series as

$$\boldsymbol{e}(t) \approx \frac{e^{\alpha}}{t}\sum_{m=1}^{K}(-1)^m \mathrm{Im}[\boldsymbol{E}(s_m)], \quad (2)$$

where α is the approximation parameter, K is the truncation number, and $s_m = (\alpha + j(m-0.5)\pi)/t$ is the sampling point in the complex frequency domain. The electric field can be computed without sequential computation because the electric field at the previous time step is not required in (2).

3 Computational Results

3.1 Verification of time-division parallel computing

To verify time-division parallel computing, the instantaneous field is obtained by FDCFD-FILT. The time response of the electric field near a metallic nanocylinder with a radius of a = 0.5 nm is analyzed. Figure 3 shows the geometry and coordinate systems. A metallic nanocylinder consists of silver, whose permittivity $\varepsilon(s)$ is described by the Lorentz–Drude model [10]. The computational area is modeled by space resolution $a/50$ and is covered by the absorbing layer. The sinusoidal plane wave with wavelength $\lambda = 350$ nm impinges along the $+x$ direction. Figure 4 shows the time response of the electric field near the cylinder. The observation point is at x = 0 and y = 0.1 nm. The FDTD and FDCFD-FILT results are in good agreement. Here, the time resolution of FDTD is set as 2×10^{-5} fs. In contrast, the time resolution of FDCFD-FILT is not restricted and is set as 0.2 fs. The relative error for the field distribution between FDCFD-FILT and FDTD is shown in Figure 5. Here, the observation time is set as t = 16 fs. In the entire computational space including the absorbing layer, the computational error is less than 0.01%. Thus, FDCFD-FILT can replace the initial fields for FDTD.

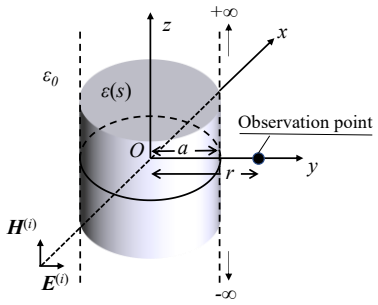

Figure 3. Geometry and coordinate systems.

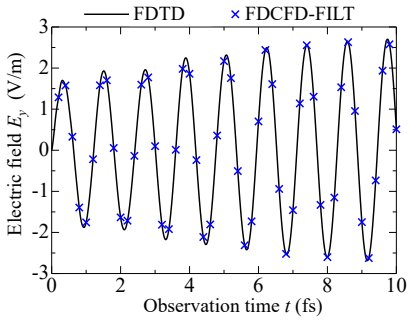

Figure 4. Comparison of FDTD and FDCFD-FILT. Both results are in good agreement.

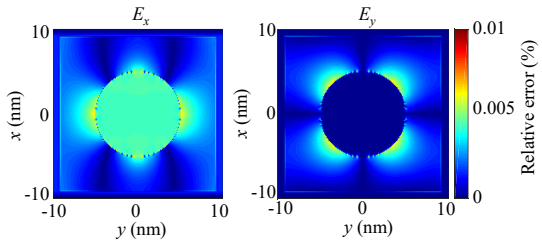

Figure 5. Relative error between FDCFD-FILT and FDTD.

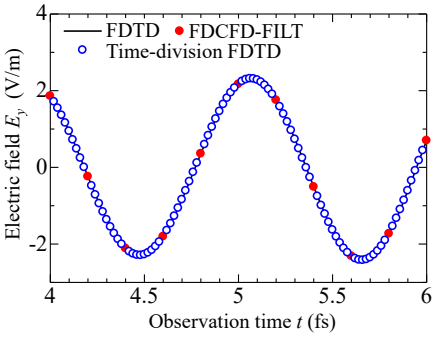

Figure 6. Time response obtained by time-division parallel computing.

3.2 Computational time of time-division parallel computing

Figure 6 shows the time response obtained by time-division parallel computing. The initial field can be updated in each processor by FDTD, because the conventional FDTD results and the proposed algorithm results are equivalent in computational accuracy. Table 1 shows a comparison of the computational time. Here, the

observation period is set as [0, 20 fs]. The number of processors is N = 10. The computational time of the conventional FDTD by one processor is about 97 minutes and that of the time-division parallel FDTD is about 23 minutes. Time-division parallel computing FDTD can be performed using FDCFD-FILT. It is based on FILT that can compute the time-domain function at a specific observation time. Data communication between processors is not required. Furthermore, the computation for the function in the time-domain and complex-frequency domain field can be decomposed into each processor [6]. Figure 7 shows the flowchart for applying the time-domain and complex-frequency domain decomposition technique to FDCFD-FILT. The computational cost of each initial field for processors can be distributed. The computational time of FDCFD-FILT is shown in Table 2. The number of processors is varied from 1 to 900. Here, the number of sampling points in the time-domain and complex-frequency domain is equal to 30. Lines 2 and 3 show the use of the time-domain decomposition, and Lines 4 and 5 indicate the complex-frequency domain decomposition. In both cases, computational time reduction can be observed upon increase in the number of processors. Lines 6, 7, and 8 show the computational cost divided in terms of the time domain and complex-frequency domain. In this case, the computational time can be reduced to 1/900 using 900 processors. Applying the time-domain division method to the previous problem, the computational time is shown in Table 3. Here, the number of time-domain divisions is 10. Compared with conventional FDTD, the computational time can be reduced to approximately 1/9 by the time-domain decomposition applied to FDCFD-FILT.

3.3 Plasmonic antennas for all-optical magnetic recording

As a realistic plasmonic device, we design plasmonic antennas for ultrafast magnetic recording systems using the time-division parallel FDTD computation. This helicity-dependent all-optical magnetic switching, as the speed of recording is 100,000 times faster than that of conventional magnetic recording [7-9]. For ultrahigh-speed and high-density recording, localized circular light is required in this system. To generate localized circularly polarized light by surface plasmon excitation, an aperture-type antenna is assumed, as shown in Figure 8. The length L and thickness w of the silver plates are 100 nm and 10 nm, respectively. The size of the aperture a is 10 nm. The incident wave is a circular polarized plane wave with wavelength $\lambda = 780$ nm and irradiates along the -z direction. The light from the outside excites the surface plasmons. In particular, the transient state of light is related to the recording speed and is investigated by the FDTD method. However, fine space resolution is required to represent the nanostructure and restrict the maximum time resolution [10]. Our method is particularly useful for the determination of the field time response in a plasmonic device design. Using time-division parallel FDTD and 30 processors, the computational time for

Table 1. Computational time for time-division parallel computing

	Computational time (s)		
	FDTD	FDCFD-FILT	Total
Conventional	5835.78	-	5835.78
Time-division FDTD	572.95	796.34	1369.29

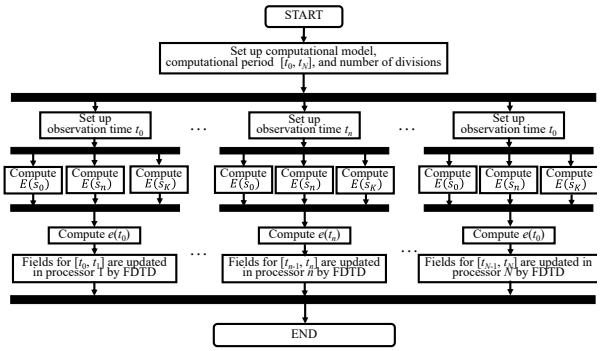

Figure 7. Flowchart for time-division parallel FDTD with time-domain and complex-frequency-domain decomposition method to FDCFD-FILT.

Table 2. Computational time for FDCFD-FILT

Number of time-domain divisions	Number of complex-frequency-domain divisions	Computational time [a.u.]
1	1	1.0000
10	1	0.1021
30	1	0.0327
1	10	0.1029
1	30	0.0341
10	10	0.0111
15	30	0.0025
30	30	0.0013

Table 3. Computational time for applying time-domain decomposition method to FDCFD-FILT.

Number of time-domain divisions	Computational time (s)		
	FDTD	FDCFD-FILT	Total
1	572.95	796.34-	1369.29
10	572.95	109.88	682.83

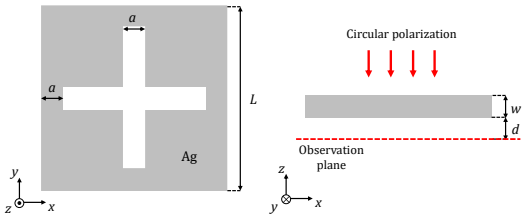

Figure 8. The aperture-type plasmonic antennas for helicity-dependent all-optical magnetic switching.

sequential part is reduced to 1/30. Applying time-domain and complex-frequency domain decomposition to FDCFD-FILT, the total computational time can be reduced to approximately 1/20. The electromagnetic field distribution is observed at a distance of 10 nm at the bottom of the antenna. To confirm the generation of circularly polarized light, intensity I and circular polarizability C are investigated, as shown in Figure 9(a) and 9(b), respectively. At the center of the aperture, the intensity is enhanced and the counterclockwise circularly

polarized light can be observed. The localized circularly polarized light is generated for high-density all-optical magnetic recording. Furthermore, the time response analysis is important for the evaluation of the recorded speed, because it is related to the generation time of the circularly polarized light. Figure 10(a) and 10(c) show the Lissajous curve and time response of the electric field at the center of the aperture, respectively. After light enters from the outside, the electric field at the center of the aperture is enhanced. Based on the time response, the x and y components of the electric field are found to be uniform in the steady state after t = 50 fs.

4 Conclusion

Time-division parallel computing FDTD has been proposed. The computational time for sequential part can be reduced to a fraction of the number of processors. Our method is based on solving the initial field of each processor obtained by FDCFD-FILT. Using time-domain and complex-frequency domain decomposition technique, the computational task of FDCFD-FILT can be divided. As a realistic application, we designed plasmonic antenna for all optical magnetic recording in significantly less time than the conventional method.

References

1. S. Ohnuki, R. Ohnishi, D. Wu, and T. Yamaguchi, "Time-division parallel FDTD algorithm," *IEEE Photon. Technol. Lett.*, **30**, 24, 2018, pp. 2143–2146, doi: 10.1109/LPT.2018.2879365

2. S. Kishimoto, S. Nishino, and S. Ohnuki, "Novel Computational Technique for Time-Dependent Heat Transfer Analysis Using Fast Inverse Laplace Transform," *Prog. In Electromagn. Res. M*, **99**, 2021, pp. 45–55 doi: 10.2528/PIERM20100203

3. D. Wu, R. Ohnshi, R. Uemura, T. Yamaguchi, and S. Ohnuki, "Finite-Difference Complex-Frequency-Domain Method for Optical and Plasmonic Analyses," *IEEE Photon. Technol. Lett.*, **30**, 11, 2018, pp. 1024–1027, doi: 10.1109/LPT.2018.2828167

4. T. Hosono, "Numerical inversion of Laplace transform and some applications to wave optics," *Radio Sci.*, **16**, 6, 1981, pp. 1015–1019, doi: 10.1029/RS016i006p01015

5. S. Masuda, S. Kishimoto, and S. Ohnuki, "Reference solutions for time-domain electromagnetic solvers," *IEEE Access*, **8**, 1, 2020, pp. 44318–44324, doi:10.1109/ACCESS.2020.2977382

6. D. Wu, S. Kishimoto, S. Ohnuki, "Optimal parallel algorithm of fast inverse Laplace transform for electromagnetic analyses," *IEEE Antennas Wireless Propag. Lett.*, **19**, 12, 2020, pp. 2018–2022, doi: 10.1109/LAWP.2020.3020327

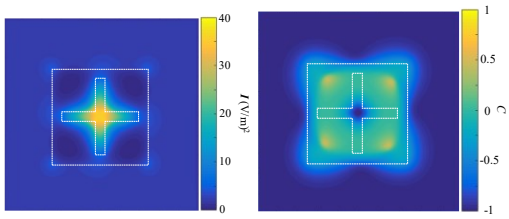

(a) (b)

Figure 9. Evaluation of localized circular polarized light. (a) Intensity I and (b) circular polarizability C.

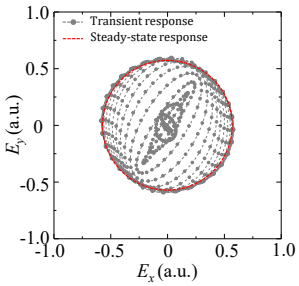

(a)

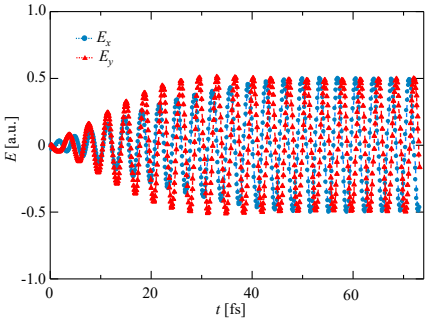

(b)

Figure 10. Time-domain analysis of electric field. (a) Lissajous curve and (b) time response

7. C. D. Stanciu, F. Hansteen, A. V. Kimel, A. Kirilyuk, A. Tsukamoto, A. Itoh, and T. Rasing, "All-optical magnetic recording with circularly polarized light," *Phys. Rev. Lett.*, **99**, 2007, pp. 047601-1–047601-4, doi: 10.1103/PhysRevLett.99.047601

8. C-H. Lambert, S. Mangin, B. S. D. Ch. S. Varaprasad, Y. K. Takahashi, M. Hehn, M. Cinchetti, G. Malinowski, K. Hono, Y. Fainman, M. Aeschlimann, and E. E. Fullerton, "All-optical control of ferromagnetic thin films and nanostructures," *Science*, **345**, 2014, pp. 1337–1340, doi: 10.1126/science.1253493

9. R. Ohnishi, K. Tatsuzawa, T. Yamaguchi, S. Kishimoto, Y. Ashizawa, K. Nakagawa, S. Ohnuki, "Robustness and Local Polarization Control of Plasmonic Antennas with Fabrication Errors," *J. Magn. Soc. Jpn.*, **44**, 4, 2020, pp. 96–101, doi: 10.3379/msjmag.2007R003

10. A. D. Rakic, A. B. Djurisic, J. M. Elazar, and M. L. Majewski, "Optical properties of metallic films for vertical-cavity optoelectronic devices," *Appl. Opt.*, **37**, 22, 1998, pp. 5271–5283, doi:10.1364/AO.37.005271